Two-Dimensional Proton NMR Studies of the Conformations and Orientations of *n*-Alkanes in a Liquid-Crystal Solvent

M. E. Rosen,† S. P. Rucker,‡ C. Schmidt,§ and A. Pines*

Materials and Chemical Sciences Division, Lawrence Berkeley Laboratory, 1 Cyclotron Road, Berkeley, California 94720, and Department of Chemistry, University of California, Berkeley, California 94720

Received: August 5, 1992; In Final Form: December 14, 1992

Magnetic dipole couplings between pairs of protons in a series of *n*-alkanes (hexane through decane) dissolved in a nematic liquid crystal were measured by two-dimensional NMR spectroscopy. The dependence of dipole couplings on the distance between pairs of protons and on the orientation of the molecule with respect to the applied magnetic field make them a potentially rich source of information about molecular conformation and orientation. Interpretation of the dipole couplings, however, is complicated by the fact that the measured couplings are averaged over all molecular conformations and orientations sampled by the molecule. Thus, the couplings do not directly provide internuclear distances and orientations, but instead provide constraints on the time-averaged conformations and orientations of the *n*-alkane molecules that can be used as a rigorous test of models for intermolecular interactions in liquid crystals. Three models for solute–liquid crystal interactions were examined; the model proposed by Photinos et al.[1] was found to be superior to the others in describing this system. The results of the modeling, including order parameters and conformer probabilities for the alkanes, are discussed and compared to *n*-alkanes in the liquid state.

1. Introduction

A large number of thermotropic nematic liquid-crystal molecules are composed of rigid, aromatic cores with flexible alkyl tails attached to one or both ends of the core. The nature of the intermolecular forces responsible for ordering in such liquid crystals is not well understood. It appears that the alkyl chains play an important role in the ordering mechanism, as is evidenced in the chain length dependence of physical properties of liquid crystals such as the nematic–isotropic transition temperature and entropy and the order parameters at different methylene sites on the chain.[2,3] Thus, an important step in the understanding of ordering in such nematic liquid crystals is the experimental characterization of the conformations and orientations of alkyl chains in liquid crystals.

Previous attempts to study chain conformation in liquid-crystal molecules or the simpler case of an *n*-alkane dissolved in a nematic liquid crystal have often employed deuterium NMR spectroscopy.[4-8] The deuterium quadrupole couplings measured in these studies provide information about the ordering of individual methylene segments in a flexible chain but provide no information about the relative positions of different methylene segments in the chain, information crucial for the detailed description of chain conformations. A potentially more useful method of measuring the conformation and orientation of alkyl chains in liquid crystals would be to use proton NMR to measure dipole couplings between pairs of protons on the chain. The proton dipole couplings are pairwise interactions that yield information not only about the ordering of each methylene segment but also about the relative positions of different methylene segments in the molecule. The form of the dipole coupling between two protons is[9]

$$\langle D_{12} \rangle = -\frac{\gamma^2 h^2}{4\pi^2}\left\langle \frac{1}{r_{12}^3}(3\cos^2\theta_{12} - 1)\right\rangle \qquad (1)$$

where γ is the gyromagnetic ratio of a proton, θ_{12} is the angle between the internuclear vector between the two protons and the applied magnetic field, r_{12} is the distance between the two protons, and the angle brackets ($\langle\ \rangle$) represent an average over the molecular motions that occur. Because of the $(3\cos^2\theta - 1)/r^3$ dependence of the dipole couplings, they should be very sensitive to molecular conformation and orientation.

Proton NMR spectra of molecules in liquid crystals, however, rapidly become intractably complex with increasing molecular size, making it virtually impossible to extract useful information from the spectra of molecules with more than a few protons. One possible method of simplifying the spectra of such molecules could be to specifically protonate a deuterated molecule at two sites. This would allow easy measurement of the dipole coupling between the two protons but would require the tedious and expensive synthesis of numerous molecules, each specifically protonated at different sites, to measure couplings between all pairs of protons on the molecule. An alternative to this has recently been devised using random (nonselective) deuteration and two-dimensional, multiple-quantum-filtered NMR.[10] This method simplifies the synthetic process considerably, requiring only one isotopic substitution reaction; then all of the proton dipole couplings can be measured in a single two-dimensional NMR experiment.

Once the dipole couplings are measured, they cannot be directly interpreted in terms of molecular conformation and orientation, since the couplings revealed in the NMR experiment are averaged over the rapid molecular motions that occur in solution. Thus the dipole couplings are averaged over all conformations and orientations sampled by the *n*-alkane molecule. To obtain useful information about conformation and orientation, the couplings must be interpreted using models for the intra- and intermolecular interactions.

In this paper we report the measurement of proton dipole couplings of a series in *n*-alkanes (hexane through decane) dissolved in a nematic liquid crystal. The detailed information about molecular conformation and orientation obtained from the experimentally measured proton dipole couplings is used to test several models for intermolecular interactions in nematic liquid crystals.

2. Experimental Section

The experimental method used to measure proton dipole couplings in flexible molecules has been described in detail

† Present address: NMR Instruments Division, Varian Associates, Inc., Palo Alto, CA 94303.
‡ Present address: Exxon Research and Engineering Co., P.O. Box 121, Linden, NJ 07036.
§ Present address: Institut für Makromolekülare Chemie, Universität Freiburg, Stefan-Meier-Str. 31, D-7800 Freiburg, FRG.
* To whom correspondence should be addressed at the Department of Chemistry.

0022-3654/93/2097-3858$04.00/0

before.[10] For the experiments in this paper, the alkanes were randomly deuterated to a level of 0.8–0.9 by gas-phase exchange with D_2 over a Pd catalyst at 90 °C. Five samples, each containing a single *n*-alkane, were prepared by dissolving a sufficient amount of the randomly deuterated alkane in the liquid-crystal Eastman Kodak EK 11650 (*p*-pentylphenyl-2-chloro(4-benzylbenzoyloxy)-benzoate) to bring the concentration of the alkane to 30 mol %. The NMR experiments were performed on a home-built 360-MHz spectrometer using the two-quantum-filtered COSY pulse sequence

$$\left(\frac{\pi}{2}\right)_\phi - \frac{t_1}{2} - (\pi)_\phi - \frac{t_1}{2} - \left(\frac{\pi}{2}\right)_\phi - \frac{\tau_1}{2} - (\pi)_x - \frac{\tau_1}{2} - \left(\frac{\pi}{2}\right)_x - \frac{\tau_2}{2} - (\pi)_x - \frac{\tau_2}{2} - t_2 \quad (2)$$

For each sample, 1024 t_2 points and 384 t_1 points were collected with a 12-kHz sweep width in both dimensions. For each t_1 point, 96 scans were averaged, cycling phase ϕ through 0°, 90°, 180°, and 270° every scan, cycling the receiver through 0° and 180° every scan, and incrementing τ_1 by 1.4 ms every fourth scan from a starting value of 1.4 ms. τ_2 was kept fixed at a value of 1.2 ms. Double-quantum deuterium decoupling[11] over a 30-kHz bandwidth was used throughout the experiments to remove proton–deuteron dipole couplings. The spectra were all recorded at a reduced temperature ($T_{red} = T/T_{N-I}$) of 0.875 to allow direct comparison of the results for different alkanes.

The peaks in the spectra appear in square patterns, from which the magnitude of the dipole couplings can be determined (neglecting *J* couplings which are not resolved in the spectra) by the relationship

$$|D| = \frac{4}{3}s - \frac{2}{3}\sqrt{s^2 + 3\Delta\nu^2} \quad (3)$$

where s is the length of the side of the square and $\Delta\nu$ is the difference in chemical shift between the two coupled protons. Increasing molecular size precludes the measurement and assignment of all dipole couplings. Fortunately, the readily resolvable couplings are those which provide the greatest constraints on molecular conformation: couplings between geminal protons, couplings involving a methyl proton, and couplings between methylene protons on second-nearest-neighbor carbons.

Assignment of the couplings to specific pairs of protons is based primarily on the chemical shifts of coupled protons, but for longer alkanes also relies on comparison with the results for *n*-hexane.[10] The sign of each coupling can be determined by assuming that the alkanes are aligned predominantly along the nematic director (along the applied magnetic field). This implies that the geminal proton couplings, with their internuclear vector approximately perpendicular to the applied magnetic field, are positive, and couplings between proton pairs whose internuclear vectors lie along the length of the chain are negative.

Figure 1 shows an example of the analysis for the two-quantum-filtered COSY spectrum of *n*-decane. The square patterns in the spectrum and their assignment to pairs of protons on the molecule are shown, with the labeling of protons given in Figure 2. Table I lists the dipole couplings obtained from this spectrum as well as those obtained from the spectra of the other *n*-alkanes in this study. Table II lists the chemical shifts of the protons on the alkanes which were used in eq 3 to calculate the dipole couplings.

3. Modeling

The proton dipole couplings listed in Table I do not provide quantitative information about molecular conformation and orientation directly but instead only give constraints on the ensemble-averaged conformations and orientations of the *n*-alkanes. To obtain quantitative information, computer simulations of the averaging process must be performed using suitable models

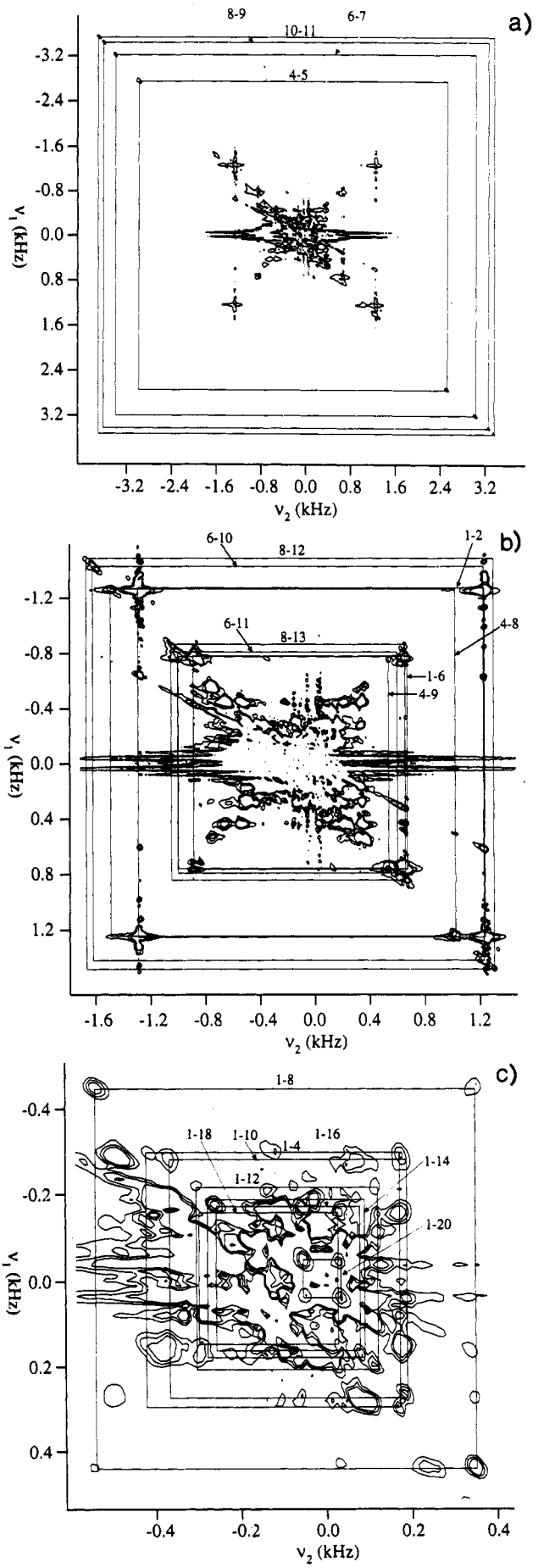

Figure 1. Proton NMR COSY spectrum of *n*-decane with the square patterns of peaks in the spectra labeled by the protons corresponding to those peaks. (a) Entire spectrum. (b) Enlarged view of spectrum. (c) Central portion of spectrum. The numbering of the protons is given in Figure 2.

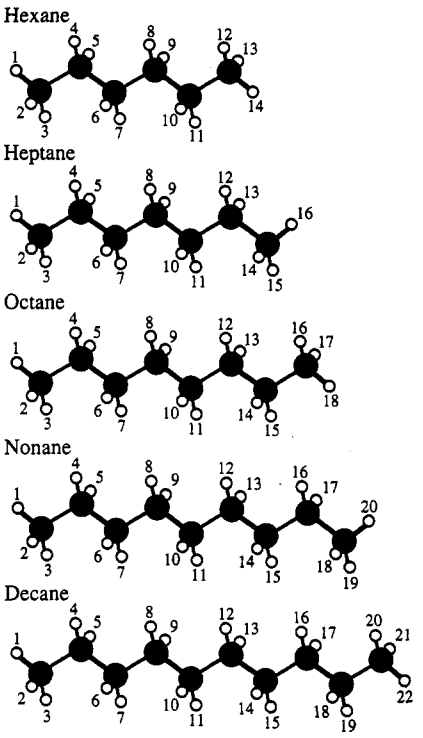

Figure 2. Numbering of the protons in the alkanes used in this study. The even-numbered protons are on the same side of the molecule, coming out of the page, and the odd-numbered protons are on the same side of the molecule going into the page.

TABLE I: Experimental Dipole Couplings

	dipole coupling[b] (Hz)				
protons[a]	hexane	heptane	octane	nonane	decane
1–2	1526	1489	1637	1546	1669
4–5	3288	3461	3539	3570	3660
6–7	3711	3897	4119	4104	4283
8–9		4093	4319	4420	4577
10–11				4220	4697
1–4	−310	−226	−319	−265	−313
1–6	−852	−916	−949	−958	−998
1–8	−484	−520	−538	−539	−556
1–10	−272	−290	−296	−300	−319
1–12	−167	−192	−204	−206	−219
1–14		−127	−129	−138	−151
1–16			−96	−93	−127
1–18				−73	−82
1–20					−57
4–8	−1323	−1453	−1544	−1554	−1666
4–9	−881	−924	−976	−977	−1020
6–10		−1575	−1710	−1721	−1863
6–11		−975	−1088	−1028	−1062
8–12				−1779	−1970
8–13				−1097	−1140

[a] Labeling of protons is given in Figure 2. [b] Experimental error ±25 Hz.

TABLE II: Experimental Chemical Shifts

	chemical shift (Hz)				
protons[a]	hexane	heptane	octane	nonane	decane
1, 2, 3	0	0	0	0	0
4, 5	219	227	229	230	230
6, 7	185	186	190	189	187
8, 9		180	177	178	174
10, 11				178	165

[a] Labeling of protons is given in Figure 2.

for the inter- and intramolecular interactions. One approach assumes a mean-field potential, $U(n,\Omega)$, for the energy of a single solute molecule in a uniaxial nematic solvent. $U(n,\Omega)$ is a function of the discrete conformations, n, of the solute molecule and the orientation, Ω, of a solute molecule–fixed axis system with respect to the nematic director. The averaged dipole coupling between two protons on this molecule can be expressed as

$$\langle D_{12} \rangle = \frac{2}{3} \sum_n p^n \sum_{\alpha\beta} S^n_{\alpha\beta} D^n_{12,\alpha\beta} \tag{4}$$

where p^n is the probability of conformer n, $S^n_{\alpha\beta}$ is the order tensor for the molecule in that conformation, and $D^n_{12,\alpha\beta}$ is the dipole coupling tensor for the two protons with the molecule in conformation n. The order tensor is defined as

$$S^n_{\alpha\beta} = \frac{1}{2}\langle 3 \cos\theta_\alpha \cos\theta_\beta - \delta_{\alpha\beta} \rangle \tag{5}$$

where θ_α ($\alpha = x, y, z$) is the angle between the director and the molecular α axis. The dipole coupling tensor for two spins-$^1/_2$ on conformer n is

$$D^n_{12,\alpha\beta} = -\frac{\gamma^2 h^2}{4\pi^2 r_{12}^3}(3 \cos\theta^{12}_\alpha \cos\theta^{12}_\beta - \delta_{\alpha\beta}) \tag{6}$$

where θ^{12}_α is the angle between the internuclear vector $\mathbf{r}_{12}$ and the molecular α axis. Since p^n and $S^n_{\alpha\beta}$ are average quantities and depend on $U(n,\Omega)$, a good choice of $U(n,\Omega)$ will allow one to simulate the experimental dipole couplings and interpret them in terms of molecular conformation and orientation.

To simplify the modeling of $U(n,\Omega)$, the solute conformer energy is assumed to be independent of its orientation. The potential $U(n,\Omega)$ can then be separated into internal (solvent-independent) and external (solute–solvent) terms:[12]

$$U(n,\Omega) = U_{\text{int}}(n) + U_{\text{ext}}(n,\Omega) \tag{7}$$

The internal part depends only on conformation and will be modeled by the rotational isomeric states (RIS) model[13] where rotation about each carbon–carbon bond is restricted to three discrete states (trans, gauche$^+$, and gauche$^-$):

$$U_{\text{int}}(n) = n_g E_g + n_{g^+g^-} E_{g^+g^-} \tag{8}$$

In the first term, n_g represents the number of gauche bonds in conformer n, and E_g the gas-phase trans–gauche energy difference (approximately 3.8 kJ/mol[14]). The second term penalizes conformations with adjacent gauche$^+$ and gauche$^-$ bonds (the pentane effect[13]), assuming the energy of this configuration, $E_{g^+g^-}$, to be 12.6 kJ/mol.[13]

The external (solute–solvent) potential can be divided into isotropic and anisotropic components:

$$U_{\text{ext}}(n,\Omega) = U^{\text{iso}}_{\text{ext}}(n) + U^{\text{aniso}}_{\text{ext}}(n,\Omega) \tag{9}$$

The isotropic, conformation-dependent component is modeled as a correction to the gas-phase trans–gauche energy difference, E_g in eq 8, due to "solvent pressure":

$$U^{\text{iso}}_{\text{ext}}(n) = n_g E^{\text{iso}}_g \tag{10}$$

though other parametrizations of this "solvent pressure" are possible. This portion of the solute–solvent potential can be combined with the internal part of the potential in eq 8 to give

$$U^{\text{iso}}(n) = n_g E^{\text{eff}}_g + n_{g^+g^-} E_{g^+g^-} \tag{11}$$

using an effective trans–gauche energy difference, $E^{\text{eff}}_g = E_g + E^{\text{iso}}_g$. The value of E^{eff}_g depends not only on the internal coordinates of the solute molecule but also on the isotropic solute–solvent interaction and determines the conformational distribution observed in solution. E^{eff}_g for liquid butane has been measured by different methods to be 2.1–2.5 kJ/mol[14] and will be used as an adjustable parameter in this study. The total potential can

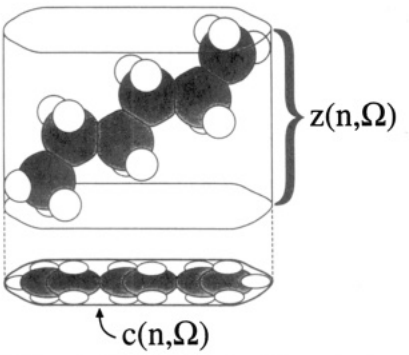

Figure 3. Model A. $z(n,\Omega)$ is the length of the projection of conformer n along the director of the liquid crystal as a function of orientation of the molecule, Ω. $c(n,\Omega)$ is the minimum circumference around the projection of the van der Waals radii of the atoms of conformer n onto a plane perpendicular to the director of the liquid crystal.

now be written

$$U(n,\Omega) = U^{iso}(n) + U^{aniso}_{ext}(n,\Omega) \tag{12}$$

where $U^{iso}(n)$ is defined by eq 11 and $U^{aniso}_{ext}(n,\Omega)$ is defined by a mean-field model for the anisotropic solute–solvent interaction. The conformer probabilities, p^n, and order tensors, $S^n_{\alpha\beta}$, can be expressed in terms of the potential $U(n,\Omega)$. p^n can be written in terms of $U(n,\Omega)$ as

$$p^n = G(n)\exp(-U^{iso}(n)/kT)Z^n_{ext}/Z_{tot} \tag{13}$$

where $G(n) = (I_xI_yI_z)^{1/2}$ is the conformer rotational kinetic energy factor[1] (which has a very small effect on the calculated probabilities), and

$$Z^n_{ext} = \int \exp(-U^{aniso}_{ext}(n,\Omega)/kT)\, d\Omega \tag{14}$$

$$Z_{tot} = \sum_n G(n)\exp(-U^{iso}(n)/kT)Z^n_{ext} \tag{15}$$

are the external and total partial functions. The average in eq 5 can be written in terms of $U^{aniso}_{ext}(n,\Omega)$:

$$S^n_{\alpha\beta} = \frac{1}{2Z^n_{ext}}\int (3\cos\theta_\alpha\cos\theta_\beta - \delta_{\alpha\beta})\exp\left(-\frac{U^{aniso}_{ext}(n,\Omega)}{kT}\right) d\Omega \tag{16}$$

In this work we test the ability of three mean-field models for the external potential $U^{aniso}_{ext}(n,\Omega)$ to describe the solute-solvent interaction. Model A introduced by van der Est, et al.[15] describes the liquid crystal solvent as an elastic continuum distorted by the presence of the solute molecule. This potential is expressed in terms of the circumference of the projection of the solute molecule onto a plane perpendicular to the nematic director:

$$U^{aniso}_{ext}(n,\Omega) = kc^2(n,\Omega) \tag{17}$$

where k is an adjustable constant describing the strength of the interaction between the solute molecule and the solvent mean field, and c is the minimum circumference[15] around the projection of the solute molecule, pictured in Figure 3. This model has also been extended by Zimmerman et al.[16] to include a term which accounts for the length of the elastic tube along the director of the liquid crystal. The potential then becomes

$$U^{aniso}_{ext}(n,\Omega) = kc^2(n,\Omega) - \zeta z(\Omega)\, c(\Omega) \tag{18}$$

where k and ζ are adjustable constants describing the strength of the solute–solvent interaction, $c(n,\Omega)$ has the same meaning as in eq 17, and $z(n,\Omega)$ is the length of the projection of the solute molecule along the liquid-crystal director, as shown in Figure 3.

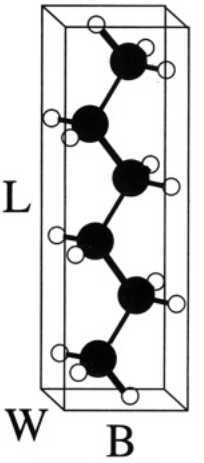

Figure 4. Model B. L, B, and W, coincident with the principal axes of the inertia tensor of an alkane conformer, are the dimensions of a parallelipeped representing that conformer.

Models B and C are based on a potential of mean torque for a solute molecule in a uniaxial mean-field. The *total* external potential, truncated to second rank, can be expressed as[3,17,18]

$$U_{ext}(n,\Omega) = u^n_{0,0}D^0_{0,0}(\Omega) + \sum_{m=-2}^{2} u^n_{2,m}D^2_{m,0}(\Omega) \tag{19}$$

where the $u^n_{l,m}$ are coefficients describing the solute–solvent interaction and the $D^l_{m,m'}(\Omega)$ are Wigner rotation matrices. The zero-rank term in eq 19 is the isotropic, conformation-dependent solute–solvent interaction, $U^{iso}_{ext}(n)$, in eq 9, and is modeled as in eq 10. The remaining second-rank terms comprise the anisotropic portion of the solute–solvent interaction:

$$U^{aniso}_{ext}(n,\Omega) = \sum_{m=-2}^{2} u^n_{2,m}D^2_{m,0}(\Omega) \tag{20}$$

Model B parametrizes the $u^n_{2,m}$ coefficients in eq 20 using a model for the solute–solvent interaction in which the interacting molecules are represented by parallelepipeds. The symmetry of a parallelepiped allows a simplification of the second rank terms[3] so that m must be even and $u^n_{2,m} = u^n_{2,-m}$, leaving

$$U^{aniso}_{ext}(n,\Omega) = u^n_{2,0}d^2_{0,0}(\beta) + 2u^n_{2,2}d^2_{2,0}(\beta)\cos(2\alpha) \tag{21}$$

The coefficients $u^n_{2,m}$ are written in terms of the length (L), width (W), and breadth (B) of the parallelepiped respresenting the solute molecule:[19,20]

$$u^n_{2,0} = (\epsilon/3)[6LBW + L(W^2 + B^2) - 2W(L^2 + B^2) - 2B(W^2 + L^2)] \tag{22}$$

$$u^n_{2,2} = (\epsilon/\sqrt{6})[(L^2 - BW)(B - W)] \tag{23}$$

The length, width, and breadth of each conformer of the molecule are calculated from the semiaxes of the ellipsoid of inertia of the conformer[20] so that L, B, and W are coincident with the principal axes of the inertia tensor of the solute molecule, pictured in Figure 4. $d^2_{0,0} = {}^1/_2(3\cos^2\beta - 1)$ and $d^2_{2,0} = \sqrt{3}/_8\sin^2\beta$ are reduced Wigner rotation matrices describing the orientation of the molecular PAS with respect to the nematic director, and ϵ is an adjustable parameter describing the strength of the solute–solvent interaction.

Model C parametrizes the $u^n_{2,m}$ as an interaction between individual carbon–carbon bonds and the nematic mean-field, and as an interaction between pairs of adjacent carbon–carbon bonds and the nematic mean field.[1] The $u^n_{2,m}$ are derived from the

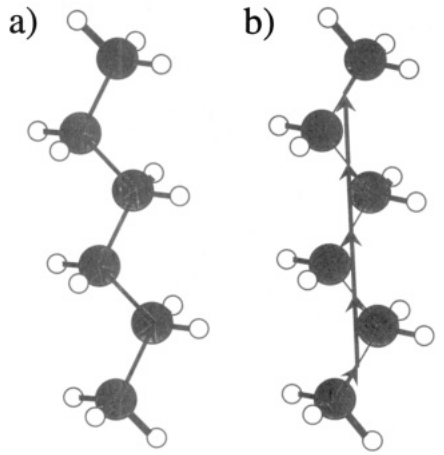

Figure 5. Model C. (a) The single carbon–carbon bond self-correlation terms of the tensor in eq 24 can be interpreted as an alignment of each carbon–carbon bond by the nematic mean field. The importance of the single bond terms is determined by the value of the multiplier of this term, $(\tilde{\omega}_1 - \bar{\omega}_0)$.[1] (b) The second sum in eq 24 can be rewritten in terms of chords connecting the midpoints of adjacent carbon–carbon bonds.[1] This term can be interpreted as the nematic mean field aligning the chords and the terminal carbon–carbon bonds. The importance of this term is determined by its coefficient, $\tilde{\omega}_1$.

Cartesian tensor:[1]

$$u_{ab} = -\frac{2}{3}\bar{\omega}_0\sum_{i=1}^{n}[3s_a^i s_b^i - \delta_{ab}\mathbf{s}^i\cdot\mathbf{s}^i] - \frac{2}{3}\tilde{\omega}_1\sum_{i}^{N-1}\left[3\left(\frac{s_a^i s_b^{i+1} + s_a^{i+1}s_b^i}{2}\right) - \delta_{ab}\mathbf{s}^i\cdot\mathbf{s}^{i+1}\right] \quad (24)$$

where N is the number of carbon–carbon bonds, $\mathbf{s}^i$ is a unit vector in the direction of carbon–carbon bond i, and s_α^i is the α (=x, y, z) component of that unit vector. The first sum in eq 24 accounts for the interaction aligning individual carbon–carbon bonds, and the second sum describes the orientation of adjacent pairs of carbon–carbon bonds by the mean field. Or, as discussed by Photinos et al.,[21] this equation can be rewritten in terms of chords connecting the midpoints of adjacent carbon–carbon bonds. In this equivalent representation, ordering of the *n*-alkane is due to alignment of individual carbon–carbon bonds and alignment of chords connecting adjacent carbon–carbon bonds, as pictured in Figure 5.

For each conformer, the tensor in eq 24 can be diagonalized, defining the molecule-fixed principal axis system (PAS) that is aligned by the liquid crystal. Expressing the interaction in this PAS makes $u_{2,1} = u_{2,-1} = 0$ and $u_{2,2} = u_{2,-2}$, so that

$$U_{\text{aniso}}^{\text{ext}}(n,\Omega) = u_{2,0}^n d_{0,0}^2(\beta) + 2u_{2,2}^n d_{2,0}^2(\beta)\cos(2\alpha) \quad (25)$$

The $u_{2,m}^n$ can then be constructed from the diagonalized Cartesian tensor of eq 24:

$$u_{2,0}^n = (1/\sqrt{6})[2u_{33} - (u_{11} + u_{22})] \quad (26a)$$

$$u_{2,2}^n = {}^1/_2(u_{11} - u_{22}) \quad (26b)$$

where u_{11}, u_{22}, and u_{33} are the principal values of that Cartesian tensor. This potential is used with either one adjustable parameter, $\bar{\omega}_0 = \tilde{\omega}_1$, or with two adjustable parameters, $\bar{\omega}_0$ and $\tilde{\omega}_1$.

To test the mean-field models, the experimental dipole couplings are simulated using the RIS model for the isotropic part of the alkane solute potential and one of the three mean-field models just described for the anisotropic part. The simulations will be done using either two or three adjustable parameters: one being the effective trans–gauche energy difference, E_g^{eff}, and the other one or two describing the strength of the solute–solvent interaction.

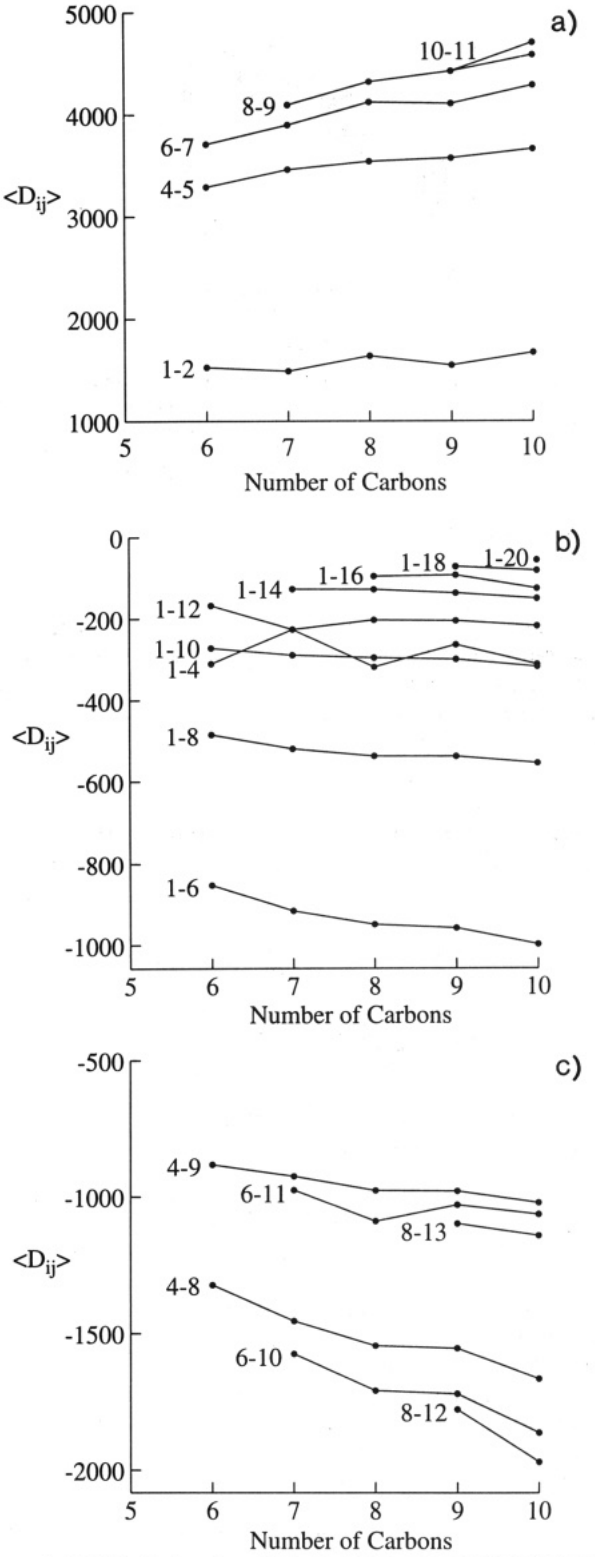

Figure 6. (a) Geminal proton dipole couplings as a function of alkane chain length. (b) Proton dipole couplings involving a methyl proton as a function of alkane chain length. (c) Dipole couplings between protons on next-nearest-neighbor carbons as a function of alkane chain length. The numbering of protons is given in Figure 2.

4. Results and Discussion

Trends in the experimental dipole couplings listed in Table I are more easily seen if the individual couplings are plotted versus chain length as in Figure 6. Figure 6a shows the geminal couplings as a function of chain length. One notable feature is the even–odd variation of the magnitude of the methyl proton couplings. This has been observed previously in a deuterium NMR study of alkyl chains dissolved in liquid crystals[20] and reflects the

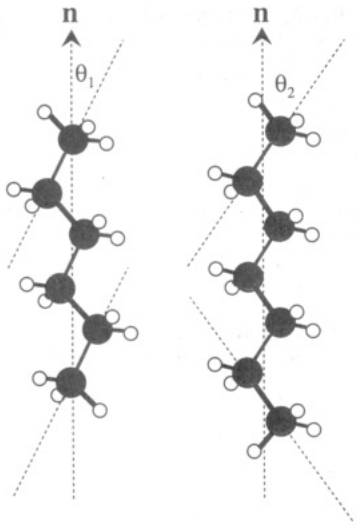

Figure 7. Even–odd variation of the dipole couplings between proton pairs 1–2 and 1–4 pictured using the lowest energy, all-trans conformations of hexane and heptane. If then it is assumed that the nematic mean field attempts to align the terminal carbon–carbon bonds, as in model C, the even alkanes with their terminal carbon–carbon bonds parallel to each other will have these bonds aligned closer to parallel to the nematic director (and the applied magnetic field) than in the odd alkanes, whose terminal carbon–carbon bonds form an angle of 112°. This makes θ_1 smaller than θ_2 and the magnitudes of the dipole couplings between proton pairs 1–2 and 1–4 larger in the even alkanes than in the odd alkanes.

difference in the shape of even and odd alkanes. If we consider the conformations of an alkane as symmetrical fluctuations about the lowest-energy, all-trans conformation, then, on average, even alkanes assume a C_{2h} symmetry and odd alkanes a C_{2v} symmetry. Looking at hexane and heptane in the all-trans conformation, as in Figure 7, it can be seen that the two terminal carbon–carbon bonds in hexane are parallel, and the terminal carbon–carbon bonds in heptane are at an angle of 112° to each other. If we assume that the liquid crystal aligns each individual carbon–carbon bond and chords plus the terminal carbon–carbon bond, as in model C, then even *n*-alkanes will have these terminal carbon–carbon bonds aligned, on average, closer to the nematic director than the terminal carbon–carbon bonds in odd *n*-alkanes. This makes the geminal methyl proton coupling larger for even *n*-alkanes than for odd *n*-alkanes.

The remaining proton dipole couplings measured in this study are shown in Figure 6b,c. These couplings provide information about molecular shape that is not available from deuterium quadrupole couplings. Figure 6b shows the dipole couplings between a methyl proton and protons on other carbon atoms in the chain. The even–odd variation in the magnitude of the coupling between a methyl proton and a proton on the neighboring carbon can be seen, again the result of the difference in ordering of terminal carbon–carbon bonds in even and odd *n*-alkanes. The effect of the $(3\cos^2\theta - 1)$ dependence of the dipole couplings can also be seen. Despite the proximity of proton 4 to the methyl protons, the coupling between this proton and the methyl protons is smaller than the coupling between the methyl protons and proton 6. This is because the internuclear vector between the methyl protons and proton 4 is closer, on average, to the magic angle (54.7°) with respect to the applied magnetic field, and the internuclear vector between the methyl protons and proton 6, which is approximately parallel to the applied magnetic field. The more distant couplings reflect the dominance of the r^{-3} dependence of the dipole couplings—the magnitudes of couplings to the methyl protons decrease as the distance of the coupling partners increases.

Figure 6c shows the couplings between protons on second-nearest-neighbor carbon atoms. There appears to be an even–odd variation in the couplings, which again can be attributed to

TABLE III: Geometrical Parameters of Alkanes

length of C–H bond	1.09 Å
length of C–C bond	1.53 Å
bond angle HCH of methylene group	109.0°
bond angle HCH of methyl group	109.47°
bond angle CCC	112°
dihedral angle for gauche conformations	±112.5°
van der Waals radius of H	1.2 Å
van der Waals radius of C	1.7 Å
mass of H	2.0
mass of C	12.0

TABLE IV: Results of Two-Adjustable-Parameter Fits to Experimental Dipole Couplings

		hexane	heptane	octane	nonane	decane
model A	k (10^{-3} N m^{-1})	3.97	3.30	2.88	2.44	2.15
	E_g^{eff} (kJ mol^{-1})	3.27	3.45	3.72	3.89	4.22
	RMS dev (Hz)	88	109	122	151	153
model B	ϵ (10^4 kJ mol^{-1} m^{-3})	2.13	1.57	1.21	0.92	0.74
	E_g^{eff} (kJ mol^{-1})	3.07	3.35	3.75	4.03	4.47
	RMS dev (Hz)	35	54	83	105	112
model C	$\tilde{\omega}_0 = \bar{\omega}_1$ (kJ mol^{-1})	0.806	0.765	0.754	0.738	0.714
	E_g^{eff} (kJ mol^{-1})	2.16	2.28	2.35	2.28	2.51
	RMS dev (Hz)	74	77	79	93	90

the difference in ordering of even- and odd-length chains, as pictured in Figure 7. Internuclear vectors between protons on second-nearest-neighbor carbons in the all-trans conformation of odd *n*-alkanes are closer to parallel to the nematic director (and the applied magnetic field) than those in even *n*-alkanes. This makes the couplings in odd *n*-alkanes larger than in even *n*-alkanes.

Simulations of the experimental dipole couplings of the alkanes were performed using the two- and three-parameter versions of the models described previously. The adjustable parameters were varied using a simplex minimization routine to optimize the root-mean-squared (RMS) difference between the calculated and experimental couplings:

$$R = \sqrt{\sum_{m=1}^{N} (D_m^{exp} - D_m^{calc})/N} \qquad (27)$$

All minimizations were performed with the alkane geometrical parameters from Table III.

The two-parameter fits used the strength of the solute–solvent interaction (k, ϵ, or $\tilde{\omega}_0$) and the effective trans–gauche energy difference (E_g^{eff}) as adjustable parameters. The RMS deviations between the calculated and experimental dipole couplings in Table IV show that all models fit the couplings of the shorter alkanes better than the longer, probably due in part to the greater number of couplings on the longer alkanes. The fits of model B for the short alkanes were superior, whereas model C provided the best fits for the long alkanes. The adjustable parameters show a variation with molecular size. The solute–solvent interaction strength parameters ϵ, k, and $\tilde{\omega}_0$, all decrease in magnitude with increasing chain length. This is countered by an increase in E_g^{eff} with increasing chain length. Both of these effects are much more pronounced in models A and B than in model C. In fact, the values of E_g^{eff} in models A and B grow larger for decane than the gas phase value of E_g^{eff} found for butane of 3.8 kJ/mol.[14] Comparison to experimentally determined values of E_g^{eff} found for butane in the liquid state (E_g^{eff} approximately 2.1–2.5 kJ/mol[14]) suggests that such large values of E_g^{eff} are physically unreasonable. While it is possible that the orienting effect of the liquid crystal might skew the conformer population distribution to favor elongated conformers, resulting in a higher E_g^{eff}, it should not be so pronounced in a "liquid-like" system such as this. Models A and B appear to work well only for small molecules, while model C appears to be adequate for all the molecules and has values of the adjustable parameters which remain relatively

TABLE V: Order Parameters from Two-Adjustable-Parameter Fits to Experimental Dipole Couplings

	S_{zz}		
	model A	model B	model C
hexane	0.19	0.17	0.19
heptane	0.21	0.19	0.22
octane	0.23	0.21	0.24
nonane	0.24	0.22	0.26
decane	0.26	0.23	0.28

TABLE VI: Conformer Probabilities from Two-Adjustable-Parameter Fits to Experimental Dipole Couplings

	total confns	no. of gauche bonds	no. of confns[a]	probabilities					
				model A		model B		model C	
				model	iso	model	iso	model	iso
hexane	27	0	1	0.27	0.29	0.28	0.27	0.20	0.19
		1	6	0.50	0.50	0.50	0.50	0.50	0.50
		2	8	0.21	0.19	0.20	0.21	0.27	0.28
		3	2	0.02	0.01	0.02	0.02	0.03	0.03
heptane	81	0	1	0.20	0.22	0.22	0.21	0.13	0.12
		1	8	0.45	0.46	0.46	0.46	0.42	0.41
		2	18	0.29	0.27	0.27	0.28	0.35	0.37
		3	12	0.05	0.05	0.05	0.05	0.09	0.10
		4	2	0.00	0.00	0.00	0.00	0.01	0.01
octane	243	0	1	0.16	0.18	0.19	0.18	0.09	0.07
		1	10	0.40	0.41	0.42	0.42	0.33	0.32
		2	32	0.33	0.31	0.30	0.31	0.39	0.40
		3	38	0.10	0.09	0.08	0.08	0.16	0.18
		4	16	0.01	0.01	0.01	0.01	0.03	0.03
		5	2	0.00	0.00	0.00	0.00	0.00	0.00
nonane	729	0	1	0.13	0.14	0.16	0.15	0.05	0.04
		1	12	0.35	0.37	0.39	0.38	0.25	0.23
		2	50	0.35	0.34	0.32	0.33	0.38	0.38
		3	88	0.14	0.13	0.11	0.12	0.24	0.26
		4	66	0.02	0.02	0.02	0.02	0.07	0.07
		5	20	0.00	0.00	0.00	0.00	0.01	0.01
		6	2	0.00	0.00	0.00	0.00	0.00	0.00
decane	2187	0	1	0.12	0.13	0.16	0.15	0.04	0.03
		1	14	0.33	0.35	0.37	0.37	0.21	0.18
		2	72	0.34	0.34	0.32	0.32	0.35	0.35
		3	170	0.17	0.15	0.13	0.13	0.28	0.29
		4	192	0.04	0.03	0.02	0.03	0.10	0.12
		5	102	0.00	0.00	0.00	0.00	0.02	0.02
		6	24	0.00	0.00	0.00	0.00	0.00	0.00
		7	2	0.00	0.00	0.00	0.00	0.00	0.00

[a] Excluding conformers with adjacent gauche$^+$ gauche bonds.

constant as the size of the alkane changes, possibly allowing prediction of dipole couplings for longer alkanes by extrapolation from the values of adjustable parameters found in the present study. Thus it appears that model C, which employs an additive potential constructed from interactions of molecular subunits with the liquid crystal mean field is preferable to models A and B, which model the overall shape of the solute molecule interacting with the liquid crystal mean field.

Having fit the dipole couplings, the models allow us to calculate order parameters and conformational probabilities for the alkanes. Table V shows the order parameters calculated using the best-fit parameters in Table IV. It can be seen that all three models give similar results for the values of the order parameters. Table VI lists the probabilities of having different numbers of gauche bonds in the chain for the different models. Alongside each probability is the probability of the conformers in an isotropic liquid with the same values of E_g^{eff} (that is, with ϵ, k, or $\bar{\omega}_0$ set to 0). It can be seen that the anisotropic solute–solvent interaction has little effect on the conformer distribution—the value of E_g^{eff} is primarily what determines the conformer distribution. This confirms the notion that the alkanes in a "liquidlike" liquid crystal such as this one behave very similarly to the neat liquid alkane, and also suggests that model A and B with their high E_g^{eff} do not provide good models for solute–solvent interaction. It can also be seen from model C that the small effect that the anisotropic solute–solvent potential does have on the conformer distribution is to favor elongated conformers slightly (e.g., all-trans, and conformers with only one gauche bond) relative to the conformer distribution in isotropic solution. From this table the probability of a given conformer can also be approximately determined, since the probabilities of conformers with a given number of gauche bonds are approximately equal regardless of the placement of the gauche bonds (excluding conformers with adjacent gauche$^+$ and gauche$^-$ bonds).

TABLE VII: Results of Three-Adjustable-Parameter Fits to Experimental Dipole Couplings

		hexane	heptane	octane	nonane	decane
model A	k (10^{-3} N m^{-1})	−3.79	−2.27	−3.86	−2.12	−2.58
	ζ (10^{-3} N m^{-1})	74.76	56.86	78.94	55.42	66.54
	E_g^{eff} (kJ mol^{-1})	1.51	1.79	0.68	1.37	0.68
	RMS dev (Hz)	56	39	66	78	77
model C	$\bar{\omega}_0$ (kJ mol^{-1})	0.970	0.914	0.914	0.907	0.855
	$\bar{\omega}_1$ (kJ mol^{-1})	0.598	0.538	0.550	0.494	0.500
	E_g^{eff} (kJ mol^{-1})	2.11	2.44	2.40	2.46	2.70
	RMS dev (Hz)	42	28	37	38	47

TABLE VIII: Order Parameters from Three-Adjustable-Parameter Fits to Experimental Dipole Couplings

	S_{zz}	
	model A	model C
hexane	0.18	0.18
heptane	0.20	0.20
octane	0.21	0.23
nonane	0.23	0.24
decane	0.24	0.26

TABLE IX: Conformer Probabilities from Three-Adjustable-Parameter Fits to Experimental Dipole Couplings

	total confns	no. of gauche bonds	no. of confns[a]	probabilities			
				model A		model C	
				model	iso	model	iso
hexane	27	0	1	0.35	0.14	0.20	0.18
		1	6	0.47	0.46	0.50	0.50
		2	8	0.17	0.35	0.27	0.28
		3	2	0.01	0.05	0.03	0.03
heptane	81	0	1	0.23	0.09	0.14	0.13
		1	8	0.45	0.37	0.43	0.42
		2	18	0.27	0.40	0.34	0.35
		3	12	0.05	0.13	0.08	0.09
		4	2	0.00	0.01	0.00	0.01
octane	243	0	1	0.23	0.02	0.09	0.08
		1	10	0.37	0.16	0.34	0.33
		2	32	0.29	0.38	0.38	0.40
		3	38	0.10	0.33	0.16	0.17
		4	16	0.02	0.10	0.02	0.03
		5	2	0.00	0.01	0.00	0.00
nonane	729	0	1	0.14	0.02	0.06	0.05
		1	12	0.34	0.14	0.26	0.25
		2	50	0.32	0.34	0.38	0.39
		3	88	0.16	0.33	0.23	0.24
		4	66	0.03	0.14	0.06	0.07
		5	20	0.00	0.02	0.01	0.01
		6	2	0.00	0.00	0.00	0.00
decane	2187	0	1	0.16	0.00	0.05	0.04
		1	14	0.29	0.05	0.22	0.20
		2	72	0.30	0.20	0.36	0.36
		3	170	0.17	0.34	0.26	0.28
		4	192	0.06	0.28	0.09	0.10
		5	102	0.01	0.10	0.02	0.02
		6	24	0.00	0.02	0.00	0.00
		7	2	0.00	0.00	0.00	0.00

[a] Excluding conformers with adjacent gauche$^+$gauche bonds.

The dipole couplings were also fit using models A and C with three adjustable parameters. Two solute–solvent interaction parameters—k and ζ for model A, or $\bar{\omega}_0$ and $\bar{\omega}_1$ for model C—and

TABLE X: Dipole Couplings for Hexane from the Three-Adjustable-Parameter Fits to the Experimental Couplings

	dipole couplings (Hz)		
protons	experiment	model A	model C
1–2	1526	1484	1616
4–5	3288	3386	3235
6–7	3711	3604	3702
1–4	−310	−262	−361
1–6	−852	−881	−836
1–8	−484	−511	−540
1–10	−272	−264	−254
1–12	−167	−160	−158
4–8	−1323	−1372	−1323
4–9	−881	−839	−907
4–6		−77	131
4–7		94	177
4–10		−751	−720
4–11		−513	−525
6–8		17	−151
6–9		104	−1

TABLE XI: Dipole Couplings for Heptane from the Three-Adjustable-Parameter Fits to the Experimental Couplings

	dipole couplings (Hz)		
protons	experiment	model A	model C
1–2	1489	1399	1504
4–5	3461	3412	3426
6–7	3897	3905	3865
8–9	4093	4135	4144
1–4	−226	−215	−289
1–6	−916	−919	−888
1–8	−520	−544	−541
1–10	−290	−278	−275
1–12	−192	−189	−182
1–14	−127	−117	−120
4–8	−1453	−1489	−1456
4–9	−924	−903	−923
6–10	−1575	−1632	−1582
6–11	−975	−924	−976
4–6		−76	25
4–7		59	111
4–10		−755	−772
4–11		−541	−526
4–12		−304	−294
4–13		−302	−289
6–8		65	17
6–9		187	114

the effective trans-gauche energy difference, E_g^{eff}, were used as adjustable parameters in the simplex minimization. Minimization with model C reached a stable minimum, but there is a range of values for the adjustable parameters in model A which result in fits of similar quality to the one shown in Table VII. This occurs because the two adjustable parameters, k and ζ, multiply the terms $c^2(\Omega)$ and $c(\Omega)\,z(\Omega)$, respectively, and $c(\Omega)$ and $z(\Omega)$ are not independent. Generally as $c(\Omega)$ decreases for a given molecule, $z(\Omega)$ increases, as shown in Figure 3. This interdependence yields a range of values for the adjustable parameters which provide fits of similar quality. Furthermore model A gives an unusually low value for E_g^{eff}. Model A is judged deficient, for while it fits the experimental couplings well, the resultant adjustable parameters seem physically unreasonable.

Model C, on the other hand, provides better fits to the dipole couplings than model A and has physically reasonable values of the adjustable parameters not very different from those found in the two-parameter fit. E_g^{eff} remains almost the same as in the two-parameter fit, and when $\bar{\omega}_0$ and $\bar{\omega}_1$ are varied independently, $\bar{\omega}_0$ is a little higher and $\bar{\omega}_1$ is a little lower than when they are varied together in the two-parameter fit. The quality of the fit using model C approaches the experimental uncertainty of the dipole couplings of ±25 Hz. It is possible to extend the model

TABLE XII: Dipole Couplings for Octane from the Three-Adjustable-Parameter Fits to the Experimental Couplings

	dipole couplings (Hz)		
protons	experiment	model A	model C
1–2	1637	1513	1683
4–5	3539	3589	3458
6–7	4119	4069	4101
8–9	4319	4353	4384
1–4	−319	−228	−359
1–6	−949	−969	−912
1–8	−538	−564	−573
1–10	−296	−301	−289
1–12	−204	−187	−200
1–14	−129	−127	−138
1–16	−96	−84	−95
4–8	−1544	−1539	−1545
4–9	−976	−941	−993
6–10	−1710	−1755	−1720
6–11	−1088	−913	−1042
4–6		−147	149
4–7		60	195
4–10		−848	−843
4–11		−552	−559
4–12		−330	−333
4–13		−307	−327
4–14		−218	−205
4–15		−210	−224
6–8		73	−106
6–9		175	46
6–12		−698	−880
6–13		−485	−587
8–10		−155	204
8–11		186	236

TABLE XIII: Dipole Couplings for Nonane from the Three-Adjustable-Parameter Fits to the Experimental Couplings

	dipole couplings (Hz)		
protons	experiment	model A	model C
1–2	1546	1392	1546
4–5	3570	3415	3490
6–7	4104	4067	4042
8–9	4420	4465	4483
10–11	4420	4536	4494
1–4	−265	−218	−300
1–6	−958	−929	−906
1–8	−539	−559	−558
1–10	−300	−290	−289
1–12	−206	−198	−198
1–14	−138	−130	−140
1–16	−93	−93	−101
1–18	−73	−65	−72
4–8	−1554	−1570	−1540
4–9	−977	−961	−957
6–10	−1721	−1835	−1735
6–11	−1028	−967	−1049
8–12	−1779	−1894	−1776
8–13	−1097	−971	−1049
4–6		−42	50
4–7		105	130
4–10		−793	−826
4–11		−554	−550
4–12		−339	−331
4–13		−325	−323
4–14		−217	−212
4–15		−214	−230
4–16		−141	−150
4–17		−140	−149
6–8		56	9
6–9		204	118
6–12		−816	−901
6–13		−505	−574
6–14		−343	−354
6–15		−323	−346
8–10		−39	62
8–11		188	151

TABLE XIV: Dipole Couplings for Decane from the Three-Adjustable-Parameter Fits to the Experimental Couplings

	dipole couplings (Hz)		
protons	experiment	model A	model C
1–2	1669	1458	1705
4–5	3660	3626	3542
6–7	4283	4298	4213
8–9	4577	4605	4617
10–11	4697	4708	4813
1–4	−313	−179	−362
1–6	−998	−995	−938
1–8	−556	−583	−560
1–10	−319	−312	−293
1–12	−219	−196	−203
1–14	−151	−135	−143
1–16	−127	−90	−105
1–18	−82	−67	−78
1–20	−57	−48	−58
4–8	−1666	−1658	−1656
4–9	−1020	−1001	−993
6–10	−1863	−1946	−1884
6–11	−1062	−991	−1070
8–12	−1970	−2026	−1958
8–13	−1140	−954	−1121
4–6		−158	157
4–7		26	203
4–10		−879	−845
4–11		−573	−536
4–12		−356	−351
4–13		−329	−340
4–14		−234	−223
4–15		−223	−236
4–16		−142	−158
4–17		−138	−157
4–18		−101	−112
4–19		−100	−112
6–8		129	−79
6–9		198	75
6–12		−736	−915
6–13		−486	−586
6–14		−374	−372
6–15		−338	−360
6–16		−206	−232
6–17		−193	−245
8–10		−141	218
8–11		200	255
8–14		−927	−959
8–15		−519	−580

and increase the number of adjustable parameters as described in ref 1, but only a slight improvement in the quality of the fits is expected.

Order parameters for the alkanes can be calculated based on the best-fit values of the three adjustable parameters and are listed in Table VIII. The values for model C are a little smaller than those shown in Table V for the two-adjustable-parameter fits, but do not differ dramatically. The conformer probabilities from model C are listed in Table IX and differ only slightly from those shown in Table VI for the two-adjustable-parameter fits.

Tables X–XIV show the individual dipole couplings calculated from the three-adjustable-parameter fits, including those predicted for the dipole couplings not measured experimentally. The relative errors in calculated dipole couplings for model C do not appear to be larger for any particular types of couplings, and it is expected that the errors in the predicted values for the dipole couplings not measured are of similar magnitude.

5. Conclusions

Proton dipole couplings on flexible molecules dissolved in liquid crystals provide detailed information about conformations and orientations. These experimental constraints provide data with which to test models for intermolecular interactions in liquid crystals. In this paper we have examined three mean-field models and found that of the three, model C proposed by Photinos et al.[1] provides the best description of the anisotropic intermolecular interaction found in liquid crystals, in agreement with results for the proton dipole couplings of hexane.[22] We also found that the RIS model with an effective trans–gauche energy difference, E_g^{eff}, of 2.1–2.7 kJ mol^{-1} adequately describes the internal degrees of freedom and the isotropic "solvent pressure" on the alkane solutes. This range of values agrees well with other experimental measurements on alkanes in the liquid state.[14] Thus we conclude that alkyl chains in the C_6–C_{10} range have conformational distributions which are not very different from those in the neat liquid.

Acknowledgment. We thank Herbert Zimmermann for the preparation of the deuterated *n*-alkane samples. M.E.R. was supported by a National Science Foundation Graduate Fellowship. This work was supported by the Director, Office of Energy Research, Office of Basic Energy Sciences, Materials Sciences Division of the U.S. Department of Energy under Contract No. DE-AC03-76SF00098.

References and Notes

(1) Photinos, D. J.; Samulski, E. T.; Toriumi, H. *J. Phys. Chem.* **1990**, *94*, 4688.
(2) Marčelja, S. *J. Chem. Phys.* **1974**, *60*, 3599.
(3) Luckhurst, G. R., Gray, G. W., Eds. *The Molecular Physics of Liquid Crystals*; Academic Press: London, 1979.
(4) Samulski, E. T.; Dong, R. Y. *J. Chem. Phys.* **1982**, *77*, 5090.
(5) Janik, B.; Samulski, E. T.; Toriumi, H. *J. Phys. Chem.* **1987**, *91*, 1842.
(6) Counsell, C. J. R.; Emsley, J. W.; Luckhurst, G. R.; Sachdev, H. S. *Mol. Phys.* **1988**, *63*, 33.
(7) Hoatson, G. L.; Bailey, A. L.; van der Est, A. J.; Bates, G. S.; Burnell, E. E. *Liq. Cryst.* **1988**, *3*, 683.
(8) Photinos, D. J.; Samulski, E. T.; Toriumi, H. *J. Phys. Chem.* **1990**, *94*, 4694.
(9) The definition of dipole coupling used here differs from the commonly used definition by a factor of 2.
(10) Gochin, M.; Pines, A.; Rosen, M. E.; Rucker, S. P.; Schmidt, C. S. *Mol. Phys.* **1990**, *69*, 671.
(11) Pines, A.; Vega, S.; Mehring, M. *Phys. Rev. B* **1978**, *18*, 112.
(12) Emsley, J. W.; Luckhurst, G. R. *Mol. Phys.* **1980**, *41*, 19.
(13) Flory, P. J. *Statistical Mechanics of Chain Molecules*; Wiley: New York, 1969.
(14) Wiberg, K. B.; Murcko, M. A. *J. Am. Chem. Soc.* **1988**, *10*, 8029 and references therein.
(15) van der Est, A. J.; Kok, M. Y.; Burnell, E. E. *Mol. Phys.* **1987**, *60*, 397.
(16) Zimmerman, D. S.; Burnell, E. E. *Mol. Phys.* **1990**, *69*, 1059.
(17) Luckhurst, G. R.; Zannoni, C.; Nordio, P. L.; Segre, U. *Mol. Phys.* **1975**, *30*, 1345.
(18) Emsley, J. W.; Luckhurst, G. R.; Stockley, C. P. *Proc. R. Soc. London, A* **1982**, *381*, 117.
(19) Straley, J. P. *Phys. Rev. A* **1973**, *10*, 1881.
(20) Janik, B.; Samulski, E. T.; Toriumi, H. *J. Phys. Chem.* **1987**, *91*, 1842.
(21) Photinos, D. J.; Samulski, E. T.; Toriumi, H. *Mol. Cryst. Liq. Cryst.* **1991**, *204*, 161.
(22) Photinos, D. J.; Poliks, B. J.; Samulski, E. T.; Terzis, A. F.; Toriumi, H. *Mol. Phys.* **1991**, *72*, 333.